



ELSEVIER

Geoderma 74 (1996) 139–160

GEODERMA

## Dissolution of a lunar basalt simulant as affected by pH and organic anions

M.J. Eick<sup>a,\*</sup>, P.R. Grossl<sup>b</sup>, D.C. Golden<sup>c</sup>, D.L. Sparks<sup>d</sup>,  
D.W. Ming<sup>c</sup>

<sup>a</sup> *Department of Agronomy, Louisiana Agriculture Experiment Station, L.S.U. Agricultural Center, Baton Rouge, LA 70803, USA*

<sup>b</sup> *Department of Plant, Soils, and Biometeorology, Utah State University, Logan, UT 84322, USA*

<sup>c</sup> *Department of Plant and Soil Sciences, University of Delaware, Newark, DE 19717, USA*

<sup>d</sup> *NASA Johnson Space Center, Mail Code SN14, Houston, TX 77058, USA*

Received 8 May 1995; accepted 10 June 1996

### Abstract

The dissolution of a lunar simulant (MLS-1) basalt was examined at 298 K; pH 3, 5, and 7; and in the presence of citrate and oxalate anions. The basalt was mined from an abandoned quarry in Duluth, Minnesota. The relative abundance of minerals in the basalt are plagioclase > pyroxene > olivine > ilmenite. The chemical composition and mineralogy of the basalt most closely resembles Apollo 11 Mare soil. For most of the experiments the order of major ion release (Mg, Ca, Fe, Al, and Si) from the MLS-1 basalt was controlled by the solubility of its mineral components. The amount of major ion release followed the order  $Fe \approx Mg > Si > Al > Ca$ . Deviations in this release order were related to the effect of the treatments on the quantity of MLS-1 basalt dissolved and the precipitation of secondary minerals. For the pH experiments dissolution followed a two-stage process. The first stage was characterized by a rapid rate of release of the major ions into solution, followed by a slower, more linear rate during the second stage. Rate coefficients were calculated from the linear portions of the rate curves and were inversely related to pH. The first stage was attributed to the dissolution of ultrafine particles created during the sample grinding process. During the second stage, dissolution occurred on the larger mineral surfaces, at higher energy sites (i.e. dislocations, twinning planes, fluid inclusions, etc). For the organic anion experiments, dissolution followed a one-stage parabolic process. Dissolution was greater in the presence of the citrate anion compared to the oxalate anion and decreased with a decrease in concentration. It is proposed that the organic anions accelerate the dissolution of the MLS-1 basalt through chemisorption and subsequent disruption of metal–oxygen

\* Corresponding author. E-mail: eick@lanmail.ocs.lsu.edu

bonds. The rate-limiting step of the reaction involves the diffusion of the cation–organic complex formed at the mineral surface.

*Keywords:* lunar simulant; basalt; organic acids; dissolution

---

## **1. Introduction**

The National Aeronautics and Space Administration (NASA) is planning further exploration of our solar system including manned missions to outer planets. A necessary first step toward this goal is to establish a manned lunar outpost. This manned lunar outpost will enable the study of the solar system unencumbered by our terrestrial atmosphere and will be a staging post for manned missions to the outer planets. To successfully establish this lunar station, it will be necessary to create a regenerative life-support system using higher plants which will require a suitable plant-growth medium. A potential problem in establishing a regenerative life-support system will be the exorbitant costs associated with transporting a terrestrial plant growth medium. An alternative material for plant growth may be the lunar regolith. The lunar regolith consists of a layer of loose, incoherent rock material that forms the majority of the Moon's surface. The finer-grained (< 1 mm) component of the lunar regolith has been loosely termed "soil" and is the result of repeated micrometeorite impacts (McKay and Ming, 1989). Lunar soil is composed of primary minerals (similar to terrestrial analogues), glasses, and other materials unique to the lunar surface. Many of the nutrients necessary for plant growth (e.g., P, Ca, Mg, S, Fe, Mn, Zn, Cu) are present in sufficient concentrations in the lunar regolith (Helmke and Corey, 1989), and those that are not can be added as fertilizers or organic amendments.

In its present state, the lunar regolith may not be an adequate plant-growth medium for several reasons. The lunar regolith is devoid of water and is extremely reduced in terms of its redox potential. Also, predominant mineral constituents are olivine and pyroxene which are among the most easily dissolved silicate minerals (Goldich, 1938). Consequently, the lunar regolith should rapidly weather when exposed to a simulated terrestrial weathering environment. Also, it has an extremely fine texture (mean grain size between 45 and 100  $\mu\text{m}$ ) which may limit proper aeration and water movement necessary for growing plants. Finally, it contains elevated concentrations of potentially toxic trace metals (i.e. Cr, Ni, and Cd) and lacks nutrient buffer and retention capacity. Therefore, it may be necessary to alter it chemically or physically to promote the initial formation of clays and hydrous oxides; which have greater nutrient retention capacities.

To assess the lunar regolith's potential as a plant-growth substrate it is necessary to understand the geochemical processes that will occur when it is subjected to an artificial weathering environment. A voluminous amount of research has been conducted on terrestrial silicate dissolution in both inorganic (Correns and Von Engelhardt, 1938; Correns, 1961, 1963; Paces, 1973; Chou and Wollast, 1984; Casey et al., 1988, 1989, Shotyk and Nesbitt, 1992) and organic solutions (Duff et al., 1963; Schalscha et al., 1967; Krumbein and Dyer, 1985; Barman et al., 1992; Franklin et al., 1994). Despite considerable research, many questions concerning terrestrial weathering and dissolution

reactions remain unresolved. Furthermore, much of this knowledge is not directly transferable to the weathering environment in a lunar regenerative life-support system. Information from terrestrial weathering studies, however, can serve as a basis for establishing experimental protocols and interpreting data obtained from dissolution studies using lunar materials.

To date, little research has been conducted on the dissolution of lunar soils (Mason et al., 1970; Keller and Huang, 1971). This may be due to the difficulty in obtaining the quantity of lunar material necessary for dissolution experiments. Lunar soil retrieved during the Apollo missions is limited in quantity and is considered a United States national treasure. Hence, NASA only dispenses small quantities (0.10 g or less) of these materials for research. Therefore, it is necessary to fabricate high-quality simulants or to obtain terrestrial analogues that have similar chemical and physical properties as the lunar regolith.

Research using lunar simulants will provide a first step in understanding geochemical processes occurring as the lunar regolith reacts with water and assessing the feasibility of using it as a plant growth substrate. Accordingly, the objectives of this study are to examine release kinetics of major ions from a lunar basalt simulant under simulated rhizospheric conditions. This involves examination of (i) basalt dissolution at pH values of 3, 5, and 7 and (ii) the influence of naturally occurring organic anions (citrate and oxalate) at pH 7.

## 2. Materials and methods

### 2.1. Solid material

A lunar basalt simulant, MLS-1, was made from components of a terrestrial basalt mined from a quarry within the city of Duluth, Minnesota. The basaltic sill intrudes

Table 1  
Bulk chemical composition of the Minnesota lunar simulant and Lunar Mare regions<sup>a</sup>

Oxide	Mass %	
	Lunar Mare	Lunar simulant (MLS-1)
SiO <sub>2</sub>	42.0	45.0
TiO <sub>2</sub>	7.5	5.2
Al <sub>2</sub> O <sub>3</sub>	13.9	15.3
FeO	15.7	14.2
Fe <sub>2</sub> O <sub>3</sub>	—	1.2
MgO	7.9	5.6
CaO	12.0	9.6
K <sub>2</sub> O	0.14	0.34
P <sub>2</sub> O <sub>5</sub>	0.12	0.45
MnO	0.21	—
Na <sub>2</sub> O	—	2.0
Cr <sub>2</sub> O <sub>3</sub>	0.30	—
Total	99.77	98.89

<sup>a</sup> Average composition of lunar mare samples.

Table 2  
Comparison of the mineral chemistry of the MLS-1 basalt and lunar mare samples

Oxide	Mass %							
	Feldspar		Pyroxene		Olivine		Ilmenite	
	Mare <sup>a</sup>	MLS-1	Mare <sup>b</sup>	MLS-1	Mare <sup>b</sup>	MLS-1	Mare <sup>b</sup>	MLS-1
SiO <sub>2</sub>	46.06	55.67	47.84	51.88	37.36	35.07	0.01	0.02
TiO <sub>2</sub>	0.15	0.09	3.46	0.64	0.11	0.07	53.58	50.05
Al <sub>2</sub> O <sub>3</sub>	33.71	28.84	4.90	1.60	0.01	0.01	0.07	0.04
FeO	0.68	0.41	8.97	11.76	27.00	40.30	44.88	45.28
MgO	0.31	0.01	14.88	13.72	35.80	23.88	2.04	1.31
CaO	18.07	10.99	18.56	19.97	0.27	—	—	0.54
K <sub>2</sub> O	0.04	0.03	—	0.01	—	0.01	—	—
MnO	0.01	—	0.25	0.29	0.22	0.49	0.40	0.50
Na <sub>2</sub> O	0.67	4.03	0.07	0.24	—	—	—	0.02
Cr <sub>2</sub> O <sub>3</sub>	—	—	0.80	0.03	0.20	—	1.08	0.07
Total	99.70	100.06	99.73	100.14	100.97	99.83	102.06	97.81

<sup>a</sup> Lunar sample 12021 (Weill et al., 1971).

<sup>b</sup> Lunar sample 74255 (Dymek et al., 1975).

anorthositic rocks of the Duluth complex comprising the mafic plutonic part of the midcontinent rift system (Weiblen and Morey, 1980). The chemical composition and mineralogy of the MLS-1 basalt were determined by electron microprobe and X-ray diffraction analyses and most closely resembles Apollo 11 Mare soil 10084 (Williams and Jadwick, 1980) (Tables 1 and 2). The relative abundance of the minerals in the MLS-1 basalt are plagioclase > pyroxene > olivine > ilmenite. The Apollo 11 mare soil 10084 exhibited a similar trend, however, pyroxene content was greater than plagioclase content (Weiblen and Gordon, 1988). The most significant differences in the major-element chemistry between lunar mare basalts and the MLS-1 basalt were the higher Na content and the presence of water and ferric iron in the MLS-1 basalt (Table 1). The bulk MLS-1 basalt was ground in a corundum grinding jar and dry sieved into eight sieve fractions to represent the grain size distribution of Apollo 11 soil 10084 (Williams and Jadwick, 1980) (Table 3). No effort was made to separate fines adhering to the grains. The basalt sample was heated to 110°C to remove adsorbed water and was stored

Table 3  
Grain size distribution of the Minnesota lunar simulant. Surface area 0.683 m<sup>2</sup>/g

Sieve size	μm	Percent by mass
> 20 mesh	> 850	7
> 35 mesh	> 500	4
> 60 mesh	> 250	8
> 100 mesh	> 150	8
> 200 mesh	> 75	16
> 270 mesh	> 53	9
> 400 mesh	> 38	16
< 400 mesh	< 38	32

in air-tight containers in an environmental glove box purged with argon gas. The initial specific-surface area was  $0.683 \text{ m}^2/\text{g}$  as determined by a three point  $\text{N}_2$  Brunauer–Emmett–Teller (B.E.T.) gas adsorption isotherm method (Table 3).

## 2.2. Reacting solutions

For the experiments conducted at pH 3 and 5, we used commercial 0.05 M biphthalate-based pH buffers (Fisher Scientific Corporation). Additionally, each buffer contained formalin to retard the growth of algae. Phthalate was chosen as the buffer because it has been shown to have little effect on silicate dissolution kinetics (Schott et al., 1981; Knauss and Wolery, 1986, 1988). The pH 7 solution was buffered using 1 mM  $\text{KHCO}_3$ . The pH of buffer solutions was adjusted using 1M HCl and the ionic strength was adjusted to approximately 0.005, 0.01, and 0.05 M with 0.1 M  $\text{NaNO}_3$ .

Solutions for the organic acid experiments were prepared using reagent-grade citric and oxalic acids (Sigma Corporation) and ultrapure water. The initial concentrations of the organic acid in the solutions were 2 and 20 mM, which were chosen to represent concentrations found in the plant-root environment (Stevenson, 1967). The pH of all organic acid solutions were adjusted to 7 with 1 M NaOH. Both citric and oxalic acid are in a fully-dissociated form at this pH. pH was maintained during the experiments by dropwise addition of 1 M NaOH or HCl. Mercuric chloride (0.02 mM) was added to each sample to prevent microbial degradation of the organic acids. The above experimental conditions are summarized in Table 4.

## 2.3. Experimental

The experiments were conducted in 500 mL acid-washed high-density polyethylene bottles. All experiments were run in duplicate. Half gram samples were added to 450 mL of reacting solution and the batch reactors were placed in an environmentally controlled incubator at  $298 \pm 1 \text{ K}$ . All batch reactors were lined with Teflon tape prior to sealing to prevent evaporation of the reacting solutions. The incubator was kept dark to prevent photo-oxidation of the organic acids. The batch reactors were gently agitated

Table 4  
Summary of experimental conditions

Solution comp.	Organic anion conc. (mM)	pH	Ionic strength (M)	Total time (days)
Biphthalate	–	3.0	0.066	365
Biphthalate	–	5.0	0.107	365
$\text{KHCO}_3$	–	7.0	0.051	365
$\text{KHCO}_3$	–	7.0	0.011	365
$\text{KHCO}_3$	–	7.0	0.006	365
Citrate	20	7.0	0.378	172
Citrate	2.0	7.0	0.040	172
Oxalate	20	7.0	0.168	172
Oxalate	2.0	7.0	0.019	172

(60 rpm) on a rotating shaker between sample collection. Approximately two hours before sampling, the solids were allowed to settle. For each analysis, 10 mL of reacting solution was withdrawn from the top of the solution column and the sample was filtered through a 0.20  $\mu\text{m}$  Gelman filter (Gelman GA-8, Gelman Sciences, Inc., Ann Arbor, MI). 10 mL of the initial solution was added back to the reaction vessel to maintain the volume and solution/solid ratios of the reaction. The pH of the filtered supernatant was decreased to approximately pH 3 using 0.5 M HCl to prevent precipitation of metals prior to analysis. Samples were analyzed for Si (0.01); (detection limits in  $\text{mg L}^{-1}$ ), Al (0.02), Ti (0.005), Fe (0.005), Mg (0.03), and Ca (0.01) by Inductively Coupled Plasma (ICP) emission spectrometry. Additionally, samples were analyzed for dissolved organic carbon using an Ionics (Watertown, MA) 1555b carbon analyzer at 24, 96, and 172 days to determine possible degradation of the organic anions.

The aqueous solution data were entered into GEOCHEM-PC (Parker et al., 1993) and MINTQA2 (Allison et al., 1991), chemical speciation programs. These programs determined the degree of saturation of ions with respect to a particular solid phase and calculated the activities of solution complexes for each experimental treatment.

#### 2.4. *Electron microscopy and electron probe microanalysis (EPMA)*

At the termination of the dissolution experiments, the weathered MLS-1 particles were filtered, rinsed twice with deionized water, air-dried, and stored in a desiccator. For scanning electron microscopy (SEM), particles from the various experiments were mounted on silver tape and glued onto Al stubs using epoxy resin. The grains were coated with carbon and examined using a JEOL JSM 35 scanning electron microscope. For electron-probe microanalysis, polished petrographic thin sections of epoxy embedded particles ( $< 1.0$  mm) were carbon coated and analyzed using a Cameca Camebax microbeam electron microprobe operated at 15 kV and 10 nA beam current. National Institute of Standards and Technology mineral standards were used for calibration.

#### 2.5. *X-ray diffraction analysis (XRD)*

The ground MLS-1 basalt was mounted in cavities carved on glass slides and analyzed by a Scintag XDS 2000 X-ray diffractometer using  $\text{Cu-K}_\alpha$  radiation; a software routine was used for  $K_\beta$  stripping.

### 3. Results

Total organic carbon analysis even after 172 days indicated less than 3% loss of dissolved carbon from the system. Therefore, little or no biotic or abiotic degradation of the organic acids to inorganic species occurred. However, this analysis measures total dissolved organic carbon which does not preclude possible bioconversion of the original organic molecule to other soluble organic species. Originally, organic acid experiments were planned to last 365 days, however, samples taken at 192 days indicated a 10% loss of dissolved organic carbon from the systems. Hence, the experiments were terminated and the data analysis was only conducted up to 172 days.

### 3.1. pH experiments

#### 3.1.1. Order of cation release

Experimental data for the quantity of Si, Al, Fe, Mg, and Ca solubilized with time at pH 3, 5 and 7 are shown in Figs. 1–3. The amount of MLS-1 basalt dissolved decreased in the order pH 3 > pH 5 > pH 7. The quantities of major elements released into solution occurred in the following order Fe  $\approx$  Mg > Si > Al > Ca for pH 3. The order was similar for the pH 5 experiment except that the quantity of Al released was nearly equal to the quantity of Fe and Mg and greater than the amount of Si. At pH 7, the order of elemental release was Ca  $\approx$  Mg > Si. Aluminum and Fe concentrations were presumably controlled by the precipitation of solid phases (gibbsite and iron oxyhydroxides) and were below ICP detection limits.

#### 3.1.2. Kinetics of dissolution

The release of Ca, Mg, Fe, Al, and Si from the MLS-1 at pH 3, 5, and 7 (Ca, Mg, and Si only) followed a two-stage process (Figs. 1–3). The first stage was characterized by a rapid release rate of these elements occurring up to 24 days ( $\sim$  600 hrs). In the second stage, the release rate of these elements declined and followed a more linear release rate until termination of the experiment (365 days). Rate coefficients, listed in Table 5, were calculated from the slope of the concentration–time curves from 24 to 365 days, except for Si which were calculated from the slope of the rate curve from 48 to 365 days. In most cases  $r^2$  values were greater than 0.91 (Table 5), except for the rate constants calculated for Al and Si, which in some cases had  $r^2$  values that were considerably

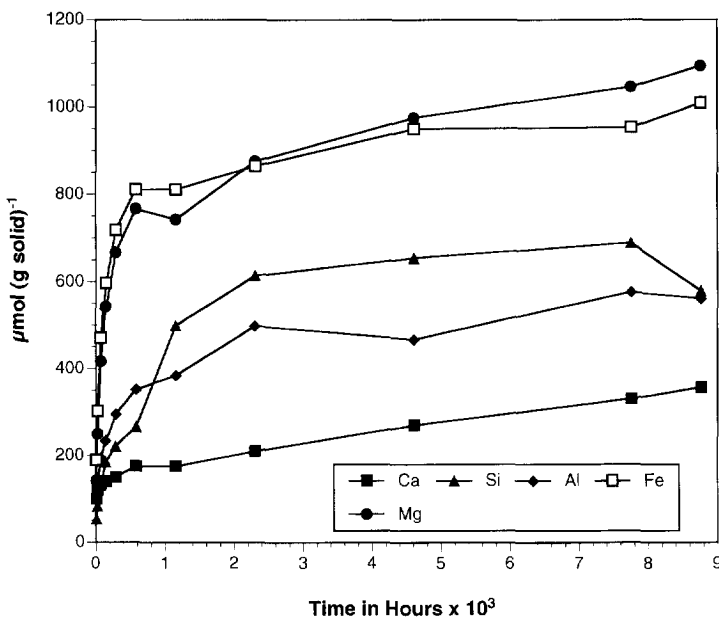


Fig. 1. Release of major ions into aqueous solution from the MLS-1 basalt as a function of time at pH 3.

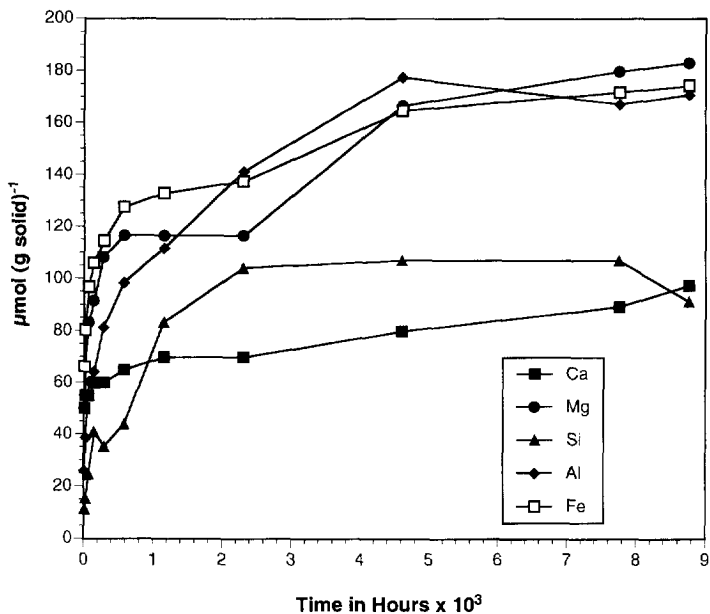


Fig. 2. Release of major ions into aqueous solution from the MLS-1 basalt as a function of time at pH 5.

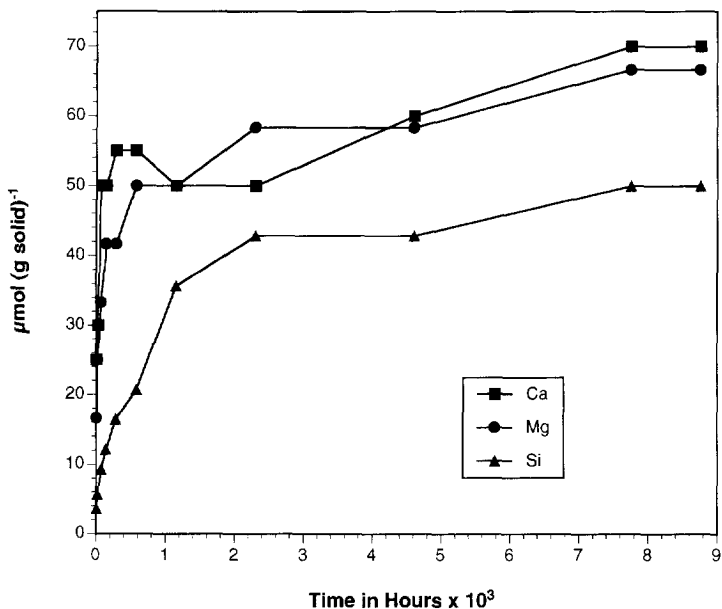


Fig. 3. Release of major ions into aqueous solution from the MLS-1 basalt as a function of time at pH 7.

Table 5

Parabolic and linear rate parameters and correlation coefficients describing major element release under the various experimental conditions for the MLS-1 basalt ( $k_p$ ,  $\mu\text{mol g}^{-1} \text{hr}^{-1/2}$ ,  $k_l$ ,  $\mu\text{mol g}^{-1} \text{hr}^{-1}$ )

Exp.	Ca			Mg			Al			Fe			Si		
	$r^2$	$k_p$	$k_l$	$r^2$	$k_p$	$k_l$	$r^2$	$k_p$	$k_l$	$r^2$	$k_p$	$k_l$	$r^2$	$k_p$	$k_l$
pH 3	0.99	–	22.7	0.95	–	41.0	0.83	–	23.9	0.92	–	22.9	0.27	–	11.3
pH 5	0.98	–	3.65	0.92	–	9.24	0.73	–	8.19	0.94	–	5.92	0.55	–	0.814
pH 7	0.88	–	2.49	0.92	–	2.07	–	–	–	–	–	–	0.89	–	1.70
pH 7	0.85	–	2.42	0.90	–	2.00	–	–	–	–	–	–	0.91	–	1.73
pH 7	0.90	–	2.40	0.88	–	2.00	–	–	–	–	–	–	0.85	–	1.75
20 mM Cit.	0.99	4.41	–	0.99	10.2	–	0.91	3.47	–	0.99	9.83	–	0.99	7.11	–
2 mM Cit.	0.98	2.22	–	0.94	6.25	–	0.89	2.34	–	0.92	6.15	–	0.95	3.69	–
20 mM Ox.	–	–	–	0.98	7.81	–	0.98	3.89	–	0.97	6.72	–	0.99	4.38	–
2 mM Ox.	–	–	–	0.88	2.57	–	0.78	2.02	–	0.40	0.280	–	0.89	2.29	–

lower. Consequently, these rate constants should be viewed with caution when making comparisons. For all elements apparent rate coefficients were inversely related to pH and decreased in the following order  $\text{Mg} > \text{Al} > \text{Fe} > \text{Ca} > \text{Si}$  (Table 5). Variations in the ionic strength at pH 7 did not affect the dissolution rate of Ca, Mg, and Si (Table 4). However, since only trace quantities of these elements were released, the effect of ionic strength on dissolution rates may not be apparent.

### 3.1.3. Chemical speciation and saturation with respect to secondary solid phases

The computer programs GEOCHEM-PC and MINTQA2 indicate that pH 3 reacting solutions were undersaturated with respect to all potential secondary solid phases. Nearly 100% of Ca, Mg, and Fe existed as free metal ions while 41% of the Al was complexed by phthalate. For the pH 5 experiments, all cations were complexed to some degree by phthalate. Aluminum was complexed to the greatest extent by phthalate (90%) followed by Fe (40%), Ca (23%), and Mg (11%). Calculations indicate that if the experiments were run in the absence of phthalate, the reacting solution at pH 5 would be supersaturated with respect to kaolinite.

### 3.1.4. Electron microscopy

Scanning electron microscopy (SEM) was used to examine weathered surfaces of the MLS-1 basalt and to determine possible precipitate formation. SEM micrographs of a clinopyroxene surface at pH 3 (Fig. 4a,b) show the classic side-by-side alignment of etch pits characteristic of weathered pyroxenes which was probably due to etching of dislocations at the boundaries of basal lamellae (Berner and Schott, 1982). The pH 5 pyroxene (Fig. 4c) exhibited similar weathering although less extensive. Similarly, the olivine particle weathered at pH 5 (Fig. 4d) showed extensive weathering and fragmentation. No secondary precipitates were observed at either pH 3 and 5 using SEM.

## 3.2. Organic acid experiments

### 3.2.1. Order of cation release

Experimental data for the quantity of Si, Al, Fe, Mg, and Ca solubilized with time for the citrate and oxalate experiments are shown in Figs. 5–8. The amount of MLS-1 basalt

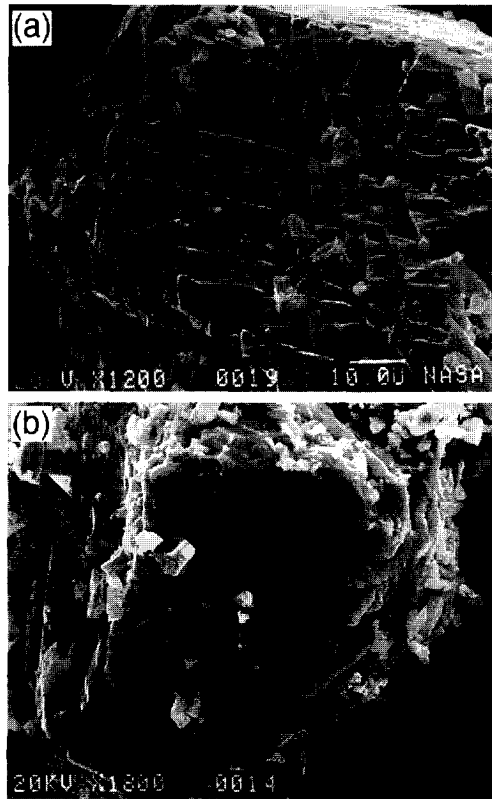


Fig. 4. Scanning electron micrographs of MLS-1 basalt weathered at pH 3 and 5. (a) Weathered clinopyroxene surface at pH 3. (b) Same as (a). (c) Weathered clinopyroxene surface at pH 5. (d) Weathered olivine surface at pH 5.

dissolved was greater for citrate than oxalate and decreased as the concentration of the organic anion decreased. The relative reactivity of the organic acids used in our study was similar to results obtained by Eick et al. (1996) for a high Ti glass, Schindler and Stumm (1987) for  $\gamma$ -alumina, Bennett et al. (1988) for quartz, and Huang and Keller (1970) for aluminosilicates. The quantities of major elements released into solution occurred in the following order  $Mg > Fe > Si > Al \approx Ca$  for citric acid experiments. The order was similar for the 20 mM oxalate experiment except that the quantity of Al released was greater than Ca. In the 2 mM oxalate experiment the quantities of major elements released into solution followed the order  $Mg > Al > Si > Ca > Fe$ . Additionally, in both oxalate experiments the net quantity of Fe released decreased with time; consistent with a reprecipitation reaction.

### 3.2.2. Kinetics of dissolution

The shape of the element release curves suggests that the dissolution of the basalt in the presence of citrate and oxalate follows a parabolic rate law (Figs. 5–8):

$$Q_i = Q_0 + k_i t^{1/2} \quad (1)$$

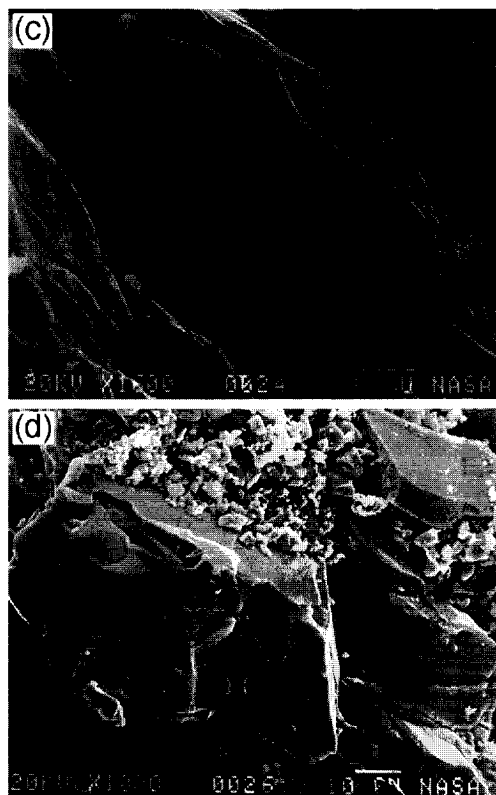


Fig. 4 (continued).

where  $Q_i$  is the amount of element released into solution ( $\mu\text{mol g}^{-1}$ ),  $k_i$  is the parabolic rate constant ( $\mu\text{mol g}^{-1} \text{hr}^{-1/2}$ ),  $Q_0$  is the quantity of mineral ( $\mu\text{mol g}^{-1}$ ) rapidly exchanged during initial wetting of the mineral surface (Grandstaff, 1978b). The parabolic rate law can be used to determine whether diffusion-controlled phenomena are rate-limiting (Sparks, 1989). A plot of the aqueous concentration of an element versus the square root of time should give a straight line with the slope of this line being the parabolic rate coefficient. Parabolic plots of major element release for citrate and oxalate are shown in Figs. 9–12. In most cases  $r^2$  values were greater than 0.97 suggesting a diffusion-controlled process. Exceptions occurred for the 2 mM oxalate experiments where all  $r^2$  values were less than 0.90. Deviations in the parabolic release occurred for the oxalate experiments at times greater than 24 days and for Ca in the 2 and 20 mM and Fe in the 2 mM experiments. Consequently, parabolic plots for these experiments were omitted.

### 3.2.3. Chemical speciation and saturation with respect to secondary solid phases

GEOCHEM-PC and MINTEQA2 calculations indicate that > 99% of the Mg, Ca, Al, and Fe were complexed with the citrate anion present at initial concentrations of 2

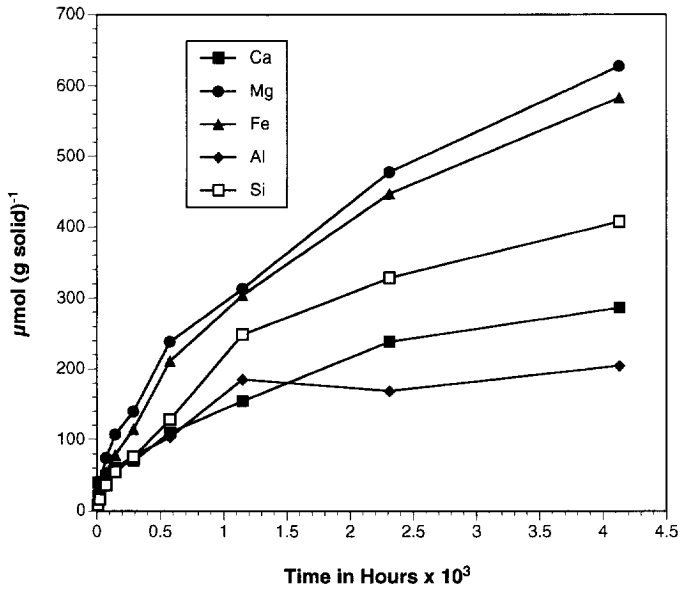


Fig. 5. Release of major ions into aqueous solution from the MLS-1 basalt as a function of time at 20 mM citrate.

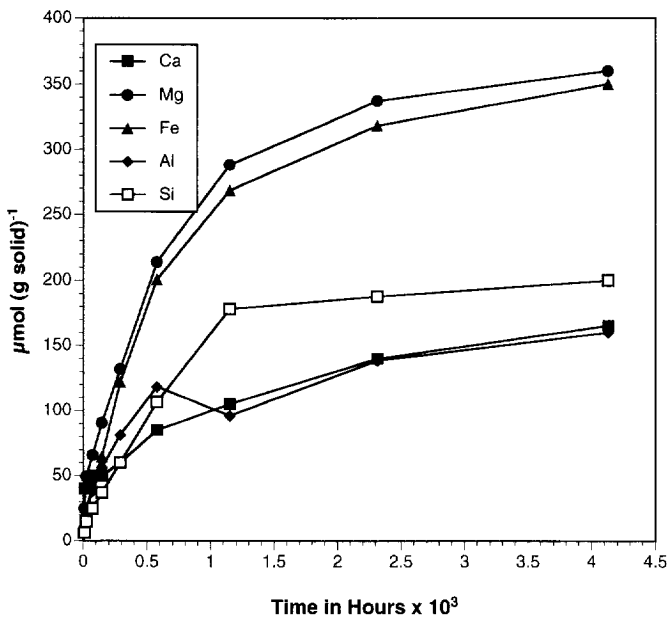


Fig. 6. Release of major ions into aqueous solution from the MLS-1 basalt as a function of time at 2 mM citrate.

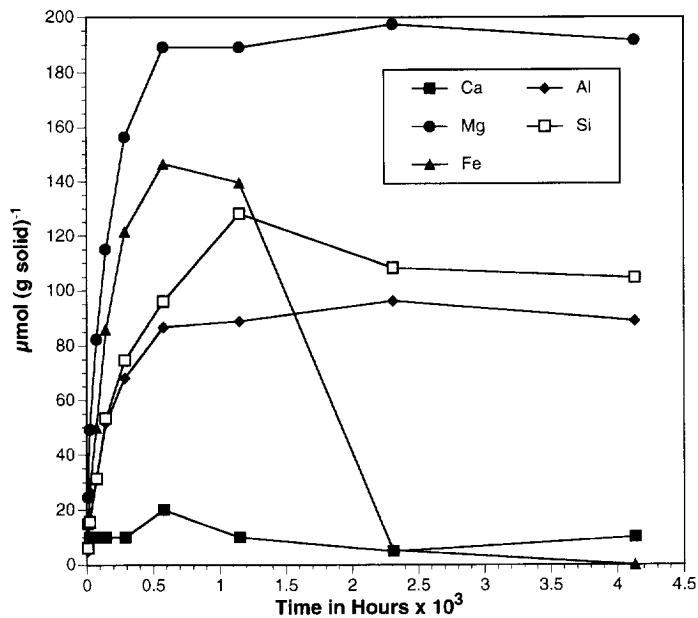


Fig. 7. Release of major ions into aqueous solution from the MLS-1 basalt as a function of time at 20 mM oxalate.

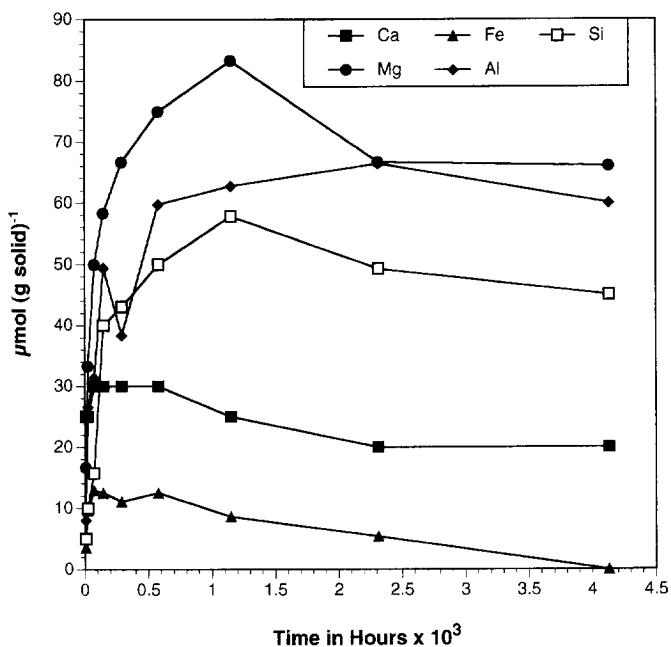


Fig. 8. Release of major ions into aqueous solution from the MLS-1 basalt as a function of time at 2 mM oxalate.

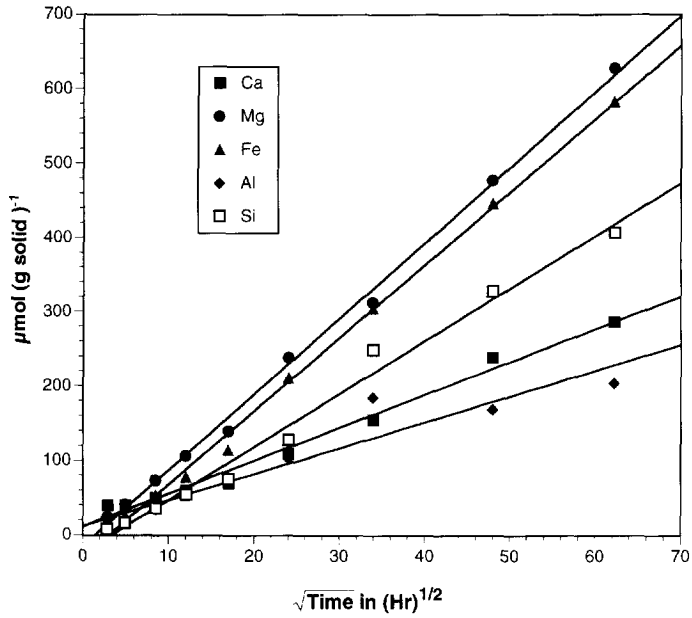


Fig. 9. Parabolic plot of major ion release into aqueous solution from the MLS-1 basalt as a function of time at 20 mM citrate.

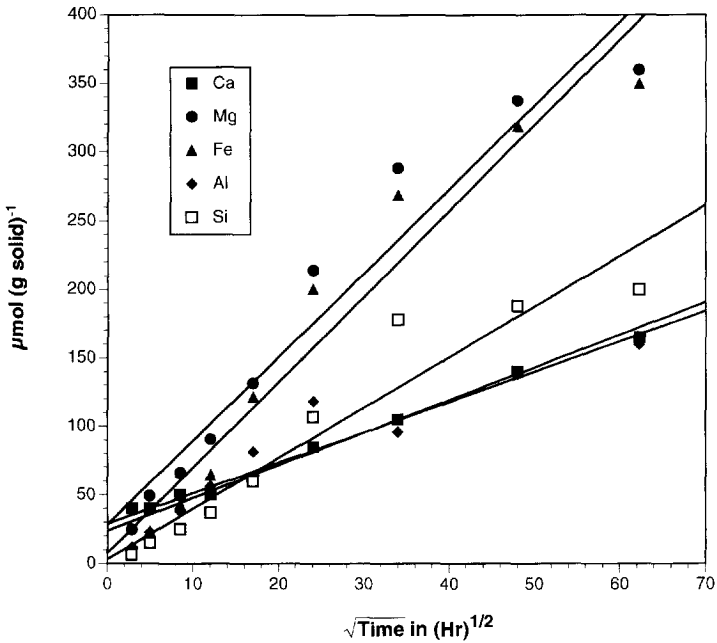


Fig. 10. Parabolic plot of major ion release into aqueous solution from the MLS-1 basalt as a function of time at 2 mM citrate.

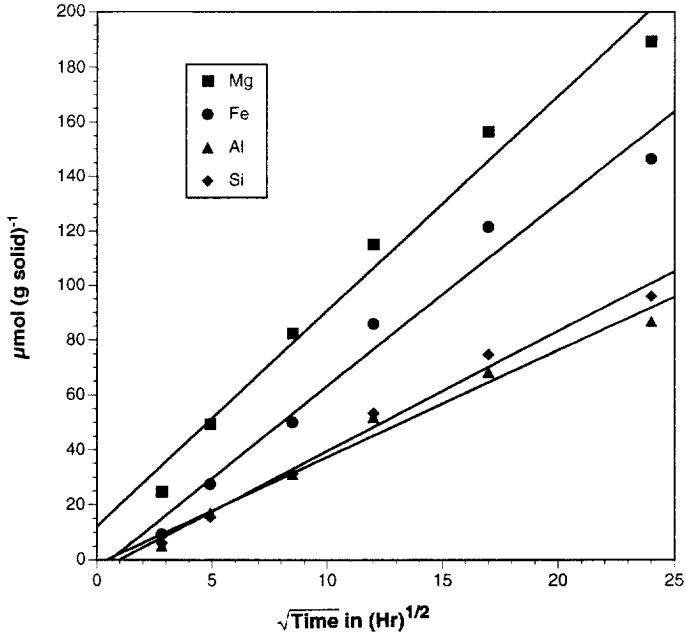


Fig. 11. Parabolic plot of major ion release into aqueous solution from the MLS-1 basalt as a function of time at 20 mM oxalate.

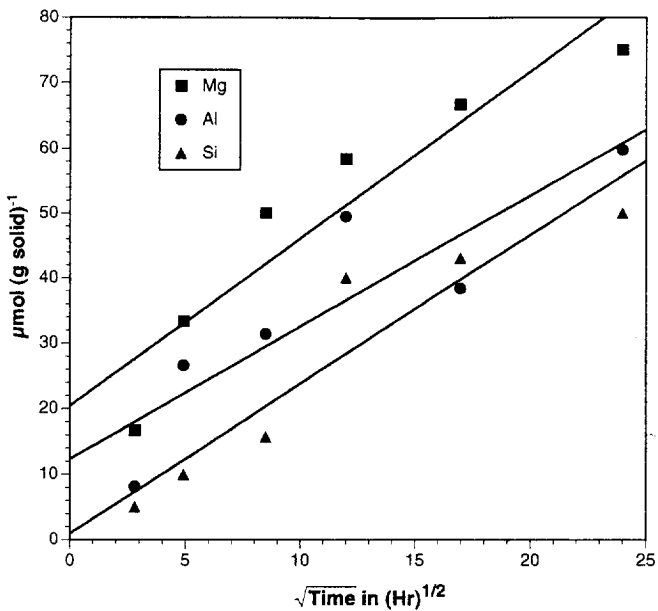


Fig. 12. Parabolic plot of major ion release into aqueous solution from the MLS-1 basalt as a function of time at 2 mM oxalate.

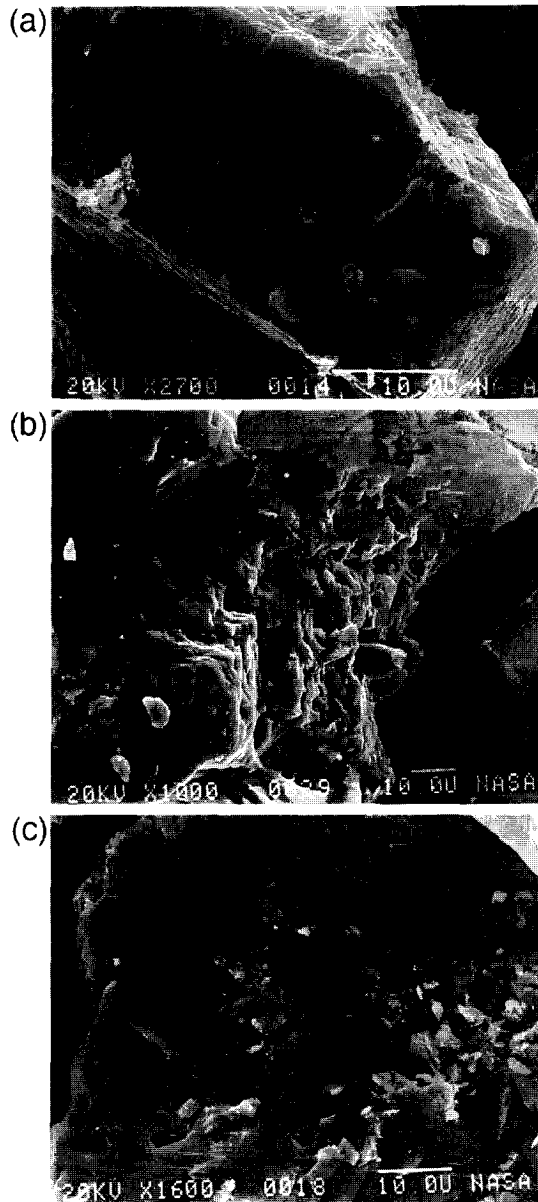


Fig. 13. Scanning electron micrographs of MLS-1 basalt weathered at 2 and 20 mM citrate and 20 mM oxalate. (a) Weathered clonopyroxene surface at 20 mM citrate. (b) Weathered olivine surface at 2 mM citrate. (c) Weathered feldspar surface at 20 mM oxalate. Precipitates (possibly Ca-oxalate) are the light colored crystal-like fragments adhering to the feldspar surface on the right-side of the micrograph.

and 20 mM. For the 20 and 2 mM oxalate experiments, > 99% of the Mg, Ca, and Al were complexed with oxalate anion while 99% of  $\text{Fe}^{+2}$  exists as the free metal. Similar results were obtained by Harrison and Thyne (1991) which showed that in aqueous solutions the divalent free  $\text{Fe}^{+2}$  ion dominated species distribution in the presence of oxalate up to and including pH 7. Computer codes also indicated that Ca-oxalate complexes will precipitate at Ca concentrations as low as 90  $\mu\text{mol}$ . Calculations run without citrate and oxalate in the reacting solutions indicate that solutions were supersaturated with respect to kaolinite.

#### 3.2.4. *Electron microscopy*

Similar to the pH experiments the pyroxene surfaces exposed to both organic acid treatments showed side-by-side etching along the boundaries of basal lamellae (Fig. 13a). The olivine grain exhibits a pitted or wavy surface (Fig. 13b) which may be the result of etching along lattice imperfections such as cleavage planes or dislocations (Grandstaff, 1978a). The feldspar surface (Fig. 13c) shows fewer weathering features than the pyroxene or olivine. Precipitates were only observed for the 20 mM oxalate experiment. Attempts to identify them using the EDAX systems failed due to their small size and destruction (suggesting Ca-oxalate) by the electron beam.

## 4. Discussion

### 4.1. *Order of cation release*

In most of the dissolution studies Fe and Mg were released in the greatest quantities followed by Si, Al, and Ca. Deviations in this release sequence occurred for the pH 5 and oxalate experiments. At pH 5 dissolution of the MLS-1 basalt was less pronounced than at pH 3 and therefore, differences in the quantity of Al, Fe, and Mg released may not be apparent. For the oxalate experiments aqueous Ca concentrations were probably controlled by the precipitation of Ca-oxalate. The order of cation release may be related to the solubility of the minerals present in the basalt which follow the sequence olivine > pyroxene > feldspar > ilmenite (proceeding from most to least soluble). Based on this solubility sequence it would be expected that Fe and Mg, major constituents of olivines and pyroxenes, would be released in the greatest amounts followed by Si, Al, and Ca. This scenario is consistent with our findings.

### 4.2. *Kinetics of dissolution*

Major element release in the pH experiments exhibited a two-stage process. The rapid release in the first stage was attributed to the fast dissolution of ultra-fine grains (Holdren and Berner, 1979; Helgeson et al., 1984) and unstable surface and subsurface features (Petrovich, 1981) created by grinding during sample preparation. These fines have a high surface area and consequently a higher free energy making them more susceptible to weathering than the bulk mineral (Holdren and Berner, 1979). Following the dissolution of these ultrafine grains the release rate became slower and followed a

more linear rate, characteristic of a surface-controlled reaction. Dissolution now occurs on the larger mineral grains at sites of excess energy (i.e. dislocations, twinning planes, step and kink structures, and grain boundaries) which were observed on SEM micrographs (Fig. 4).

The mechanism of silicate dissolution at reduced pH values is initiated by hydrogen ions which are involved in diffusion exchange with cations and surface protonation reactions. These protonation reactions weaken the metal oxygen bonds which enhances the release of Si from the surface. Hence, as the pH is reduced the dissolution of the silicate mineral increases (Stumm and Wieland, 1990). A plot of  $\log(\text{rate})$  versus pH often results in a linear relationship over certain pH values depending on the type of mineral. For our experiments, there was no linear relationship between Si release rates and the activity of  $\text{H}^+$  over the pH range of 3–7. This may be due to both a pH-dependent and -independent reaction occurring in this pH range. These results are consistent with Amrhein and Suarez (1988) who examined the affect of pH on the dissolution of anorthite and observed both a pH-dependent ( $\text{pH} < 4.7$ ) and -independent ( $\text{pH} > 4.7$ ) dissolution rate.

The rate coefficients for Si released at pH 3 and 5 were compared to those obtained by Schott et al. (1981) for the pyroxene diopside. The rates ( $-\log k$  in moles  $\text{g}^{-1} \text{sec}^{-1}$ ) obtained by Schott et al. (1981) were 9.2 and 10.8 at pH 3 and 5 while rates obtained for the MLS-1 simulant (converted to moles  $\text{g}^{-1} \text{sec}^{-1}$ ) were 8.5 and 9.7 at pH 3 and 5, respectively. Considering the presence of other minerals in the MLS-1 simulant which will affect the overall release rate of Si, the calculated rate coefficients suggest that pyroxenes present in the MLS-1 basalt exert a major influence on the observed order and rate of major element release.

The observed parabolic time dependence of major element release observed in the organic acid experiments indicates a rate-determining step involving diffusion. We propose that the organic acids accelerate the dissolution through chemisorption of the organic ligands on the basalt surface. The adsorbed organic ligand is a  $\pi$  donor and shifts electron density inward toward the framework of the mineral. This charge transfer increases the electron density of the metal–oxygen bond which weakens the framework of the mineral. These bonds are now more susceptible to hydrolysis increasing the rate of dissolution (Eick et al., 1996). Similar to Barman et al. (1992), it is proposed that the rate-limiting step involves diffusion of this cation–organic complex which is formed at the surface of the mineral. Although it should be noted that the basalt consists of many minerals and the observed rates of major element release and proposed dissolution mechanisms may be much more complex (Schott and Petit, 1987).

#### 4.3. *Chemical speciation and saturation with respect to secondary solid phases*

MINTEQA2 and GEOCHEM-PC were used to calculate saturation indices with respect to secondary solid phases. As would be expected at pH 3, reacting solutions were undersaturated with respect to all secondary solid phases. Above a pH of approximately 4.0, the aqueous concentration of Al is predicted to be controlled by the precipitation of microcrystalline gibbsite. Eventually, as the aqueous concentration of Si increases, reacting solutions approach the stability field of kaolinite, and at pH 5, calculations predict that reacting solutions are supersaturated with respect to kaolinite.

Similarly, organic anion reacting solutions are supersaturated with respect to kaolinite. The oxalate experiments show a drop in the aqueous Fe concentration toward the end of the experiment and GEOCHEM-PC results predict that in the presence of oxalate, the  $\text{Fe}^{2+}$  ion dominant Fe species. Since no attempt was made to purge oxygen from the reacting solutions,  $\text{Fe}^{2+}$  should oxidize with time and precipitate as an Fe(III) oxyhydroxide. The precipitation of  $\text{Fe}^{3+}$  as an iron oxyhydroxide has been observed to scavenge other elements from solution which may explain the non-parabolic release of major elements at time periods greater than 24 days for both oxalate experiments (Siever and Woodford, 1979).

In addition to basalts the lunar regolith is composed of a variety of materials that may weather more rapidly (i.e. glasses). Consequently, under artificial weathering environments solution compositions will be much more complex than observed during the dissolution of the MLS-1 basalt. Also, dissolution rates can be increased chemically to speed the formation of secondary weathering products with significant cation exchange capacity. For example, under mild hydrothermal conditions Ming and Lofgren (1990) observed the formation of ion-exchange minerals (zeolites and smectites) from a synthetic lunar basaltic glass. Although in the above experiments solution compositions were supersaturated with respect to kaolinite, based on kinetics it would be unlikely that this solid phase would precipitate during initial weathering of the lunar regolith. Future dissolution studies are necessary using additional simulants and actual lunar minerals in order to determine potential formation of high ion-exchange minerals.

#### *4.4. Implications for use as a plant growth substrate*

Reductions in pH and the release of organic ligands will rapidly weather unstable basalt minerals and release ample quantities of the plant nutrient elements Ca, Mg, and Fe. Under intensively cropped systems, such as those necessary in a regenerative life support system, it is likely that organic acids will be found at greater concentrations than in terrestrial cropping systems. The above results indicate that organic anions may limit the precipitation of secondary minerals through complexation reactions. Furthermore, organic acids have been known to inhibit precipitation of soil minerals by poisoning crystal growth (Inskeep and Silvertooth, 1988; Grossl and Inskeep, 1991). Therefore, organic acids should play a dominant role in weathering and precipitation reactions in the regenerative life support system. The success of the lunar regolith as a plant growth medium will rely on the production of secondary minerals with significant nutrient supplying/retention capacity. Plant nutrient elements not supplied by the lunar regolith may be added as fertilizer and organic amendments. The high solubility of lunar minerals similar to those present in the MLS-1 basalt should lead to development of secondary mineral phases with significant cation exchange capacity. Additionally, monitoring solution composition and adjusting it through artificial inputs will allow one to induce the formation of secondary mineral phases. Understanding the geochemistry of lunar regolith components under artificial weathering environments is necessary for assessing its potential as a plant growth substrate. Studies using lunar simulants will provide the first step in achieving this goal.

## 5. Summary and conclusions

The dissolution of the MLS-1 simulant is accelerated at reduced pH and in the presence of the citrate and oxalate anions. The amount of cations released from the MLS-1 basalt followed the general sequence  $Fe \approx Mg > Si > Al \approx Ca$  which is related to the solubility of the minerals present in the basalt (olivine > pyroxene > feldspar > ilmenite). The kinetics of dissolution of the MLS-1 basalt in the pH experiments follows a two stage process. The first stage is characterized by a rapid release of major elements and is due to the dissolution of ultra-fine grains created during sample grinding. After depletion of these ultrafine grains, release of major elements is linear and characteristic of a surface controlled reaction. Reacting solutions were undersaturated with respect to all secondary solid phases in the pH 3 experiments. In contrast the reacting solutions in the pH 5 experiments were saturated with respect to kaolinite.

Dissolution of the basalt in the presence of the organic acids followed parabolic kinetics indicating a diffusion controlled process. It is proposed that the rate limiting step is the diffusion of the cation–organic complex which is formed at the surface of the mineral. Similar to the pH 5 experiments, reacting solutions for the organic acid experiments were supersaturated with respect to kaolinite. In the oxalate experiments, Ca concentrations were controlled by the precipitation of Ca-oxalate; and the aqueous concentration of iron decreased toward the end of the experiment due to the precipitation of iron oxyhydroxides.

## Acknowledgements

This research was supported by NASA's Graduate Student Researchers Program. Thanks are extended to NASA and the personnel at the Lyndon B. Johnson Space Center for the use of their facilities for conducting part of this research. We would also like to thank the constructive and helpful reviews of two anonymous reviewers which significantly improved the manuscript.

## References

- Allison, J.D., Brown, D.S. and Novo-Gradac, K.J., 1991. MINTEQA2/PRODEFA2, a geochemical assessment model for environmental systems: version 3.0 user's guide. Environmental Research Laboratory Office of Research and Development. U.S. EPA, Athens, GA.
- Amrhein, C. and Suarez, D.L., 1988. The use of a surface complexation model to describe the kinetics of ligand-promoted dissolution of anorthite. *Geochim. Cosmochim. Acta*, 52: 2785–2793.
- Barman, A.K., Varadachari, C. and Ghosh, K., 1992. Weathering of silicate minerals by organic acids. I. Nature of cation solubilisation. *Geoderma*, 53: 45–63.
- Bennett, P.C., Melcer, M.E., Siegel, D.I. and Hassett, J.P., 1988. The dissolution of quartz in dilute aqueous solutions of organic acids at 25°C. *Geochim. Cosmochim. Acta*, 52: 1521–1530.
- Berner, R.A. and Schott, J., 1982. Mechanism of pyroxene and amphibole weathering. II. Observations of soil grains. *Am. J. Sci.*, 282: 1214–1231.
- Casey, W.H., Westrich, H.R. and Arnold, G.W., 1988. Surface chemistry of labradorite feldspar reacted with aqueous solutions at pH = 2, 3 and 12. *Geochim. Cosmochim. Acta*, 52: 2795–2807.

- Casey, W.H., Westrich, H.R., Arnold, G.W. and Banfield, J.F., 1989. The surface chemistry of dissolving labradorite feldspar. *Geochim. Cosmochim. Acta*, 53: 821–832.
- Chou, L. and Wollast, R., 1984. Study of the weathering of albite at room temperature and pressure with a fluidized bed reactor. *Geochim. Cosmochim. Acta*, 48: 2205–2217.
- Correns, C.W., 1961. The experimental chemical weathering of silicates. *Clay Miner. Bull.*, 4: 249–281.
- Correns, C.W., 1963. Experiments on the decomposition of silicates and discussion of chemical weathering. *Clays Clay Miner.*, 10: 443–459.
- Correns, C.W. and Von Engelhardt, W., 1938. Neue Untersuchungen ueber die Verwitterung des Kalifeldspates. *Chem. Erde*, 12: 1–22.
- Duff, R.B., Webley, D.M. and Scott, R.O., 1963. Solubilization of minerals by 2-ketogluconic acid-producing bacteria. *Soil Sci.*, 95: 105–114.
- Dymek, R.F., Albee, A.L. and Chodos, A.A., 1975. Comparative mineralogy and petrology of Apollo 17 basalts: Samples 70215, 71055, 74255 and 75055. In: *Proc. 4th Lunar Sci. Conf.*, Vol. 1, pp. 925–931.
- Eick, M.J., Grossl, P.R., Golden, D.C., Sparks, D.L. and Ming, D.W., 1996. Dissolution kinetics of a lunar glass simulant at 298 K. The effect of pH and organic acids. *Geochim. Cosmochim. Acta*, 56: 157–170.
- Franklin, F.P., Hajash, A., Dewers, T.A. and Tieh, T.T., 1994. The role of carboxylic acids in albite and quartz dissolution; An experimental study under diagenetic conditions. *Geochim. Cosmochim. Acta*, 58: 4259–4279.
- Goldich, S.S., 1938. A study in rock-weathering. *J. Geol.*, 46: 17–58.
- Grandstaff, D.E., 1978a. Some kinetics of bronzite orthopyroxene dissolution. *Geochim. Cosmochim. Acta*, 42: 1097–1103.
- Grandstaff, D.E., 1978b. Changes in surface area and morphology and the mechanism of forsterite dissolution. *Geochim. Cosmochim. Acta*, 42: 1899–1901.
- Grossl, P.R. and Inskeep, W.P., 1991. Precipitation of dicalcium phosphate dihydrate in the presence of organic acids. *Soil Sci. Soc. Am. J.*, 55: 667–675.
- Harrison, W.J. and Thyne, G.D., 1991. Predictions of diagenetic reactions in the presence of organic acids. *Geochim. Cosmochim. Acta*, 56: 565–586.
- Helgeson, H.C., Murphy, W.M. and Aagaard, P., 1984. Thermodynamic and kinetic constraints on reaction rates among minerals and aqueous solutions. II. Rate constants, effective surface area and the hydrolysis of feldspar. *Geochim. Cosmochim. Acta*, 48: 2405–2432.
- Helmke, P.A. and Corey, R.B., 1989. Development of lunar-derived soils. In: D.W. Ming and D.L. Henninger (Editors), *Lunar Based Agriculture, Soils for Plant Growth*. Soil Science Society of America, Madison, WI, pp. 193–212.
- Holdren, G.R., Jr. and Berner, R.A., 1979. Mechanism of feldspar weathering. I. Experimental studies. *Geochim. Cosmochim. Acta*, 43: 1161–1171.
- Huang, W.H. and Keller, W.D., 1970. Dissolution of rock-forming silicate minerals in organic acids: simulated first-stage weathering of fresh mineral surfaces. *Am. Mineral.*, 57: 2076–2094.
- Inskeep, W.P. and Silvertooth, J.C., 1988. Inhibition of hydroxyapatite precipitation in the presence of fulvic, humic and tannic acids. *Soil Sci. Soc. Am. J.*, 52: 941–946.
- Keller, W.D. and Huang, W.H., 1971. Response of Apollo 12 lunar dust to reagents simulative of those in the weathering environment of Earth. *Proceedings of the Second Lunar Science Conference*, Vol. 1. M.I.T. Press, Cambridge, MA, pp. 973–981.
- Knauss, K.G. and Wolery, T.J., 1986. Dependence of albite dissolution kinetics on pH and time at 25°C and 70°C. *Geochim. Cosmochim. Acta*, 50: 2481–2497.
- Knauss, K.G. and Wolery, T.J., 1988. The dissolution kinetics of quartz as a function of pH and time at 70°C. *Geochim. Cosmochim. Acta*, 52: 43–53.
- Krumbein, W.E. and Dyer, B.D., 1985. The plant is alive — weathering and biology, a multi-faceted problem. In: J.I. Drever (Editor), *The Chemistry of Weathering*. Reidel New York, pp. 143–160.
- Mason, B., Fredriksson, K., Henderson, E.P., Jarosewich, E., Melson, W.G., Towe, K.M. and White, J.S., 1970. Mineralogy and petrology of lunar samples. *Science*, 167: 656–659.
- McKay, D.S. and Ming, D.W., 1989. Mineralogical and chemical properties of the lunar regolith. In: D.W. Ming and D.L. Henninger (Editors), *Lunar Based Agriculture, Soils for Plant Growth*. Soil Science Society of America, Madison, WI, pp. 45–68.

- Ming, D.W. and Lofgren, G.E., 1990. Crystal morphologies of minerals formed by hydrothermal alteration of synthetic lunar basaltic glass. In: L.A. Douglas (Editor), *Soil Micromorphology: A Basic and Applied Science*. Elsevier, Amsterdam, pp. 463–470.
- Paces, T., 1973. Steady-state kinetics and equilibrium between groundwater and granitic rock. *Geochim. Cosmochim. Acta*, 37: 2641–2643.
- Parker, D.R., Norvell, W.A. and Chaney, R.L., 1993. GEOCHEM-PC: A chemical speciation program for IBM and compatible computers. In: R.H. Loeppert (Editor), *Soil Chemical Equilibrium and Reaction Models*. Soil Science Society of America, Madison, WI.
- Petrovich, R., 1981. Kinetics of dissolution of mechanically comminuted rock-forming oxides and silicates I. Deformation and dissolution of oxides and silicates in the laboratory and at the earth's surface. *Geochim. Cosmochim. Acta*, 45: 1675–1686.
- Schalscha, E.B., Appelt, H. and Schatz, A., 1967. Chelation as a weathering mechanism — I. Effect of complexing agents on the solubilization of iron from minerals and granodiorite. *Geochim. Cosmochim. Acta*, 31: 587–596.
- Schindler, P.W. and Stumm, W., 1987. The surface chemistry of oxides, hydroxides and oxide minerals. In: W. Stumm (Editor), *Aquatic Surface Chemistry*. Wiley, New York, pp. 83–110.
- Schott, J. and Petit, J.C., 1987. New evidence for the mechanisms of dissolution of silicate minerals. In: W. Stumm (Editor), *Aquatic Surface Chemistry*. Wiley, New York, pp. 293–315.
- Schott, J., Berner, R.A. and Sjöberg, E.L., 1981. Mechanisms of pyroxene and amphibole weathering. I: Experimental studies of iron-free minerals. *Geochim. Cosmochim. Acta*, 45: 2133–2135.
- Shotyk, W. and Nesbitt, H.W., 1992. Incongruent and congruent dissolution of plagioclase feldspar: effect of feldspar composition and ligand complexation. *Geoderma*, 55: 55–78.
- Siever, R. and Woodford, N., 1979. Dissolution kinetics and weathering of mafic minerals. *Geochim. Cosmochim. Acta*, 43: 717–724.
- Sparks, D.L., 1989. *Kinetics of Soil Chemical Processes*. Academic Press, New York, pp. 26–28.
- Stevenson, F.J., 1967. Organic acids in soils. In: A.D. McLaren and G.H. Petersen (Editors), *Soil Biochemistry*, Vol. 1. Academic Press, New York, pp. 110–146.
- Stumm, W. and Wieland, E., 1990. Dissolution of oxide and silicate minerals: Rates depend on surface speciation. In: W. Stumm (Editor), *Aquatic Chemical Kinetics*. Wiley, New York, pp. 367–400.
- Weiblen, P.W. and Morey, G.B., 1980. A summary of the stratigraphy, petrology and structure of the Duluth complex. *Am. J. Sci.*, 280-A: 88–133.
- Weiblen, P.W. and Gordon, K.L., 1988. Characteristics of a simulant for lunar surface materials. In: *Lunar Base Symposium*, April, 1988, Houston, TX. Paper No. LBS-88-213.
- Weill, D.F., Grieve, R.A., McCallum, I.S. and Bottinga, Y., 1971. Mineralogy–petrology of lunar samples. Microprobe studies of samples 12021 and 12022: viscosity of melts of selected lunar compositions. In: *Proc. 2nd Lunar Sci. Conf.*, Vol. 1, pp. 413–430.
- Williams, R.J. and Jadwick, J.J., 1980. *Handbook of lunar materials*. NASA Ref. Publ. 1057. Natl. Tech. Info. Serv., Springfield, VA.